PHYSICAL REVIEW E **95**, 060201(R) (2017)

From bulk self-assembly to electrical diffuse layer in a continuum approach for ionic liquids: The impact of anion and cation size asymmetry

Sariel Bier,[1] Nir Gavish,[2,*] Hannes Uecker,[3] and Arik Yochelis[1,†]

[1]*Department of Solar Energy and Environmental Physics, Swiss Institute for Dryland Environmental and Energy Research, Blaustein Institutes for Desert Research (BIDR), Ben-Gurion University of the Negev, Sede Boqer Campus, 8499000 Midreshet Ben-Gurion, Israel*

[2]*Department of Mathematics, Technion–IIT, 3200003 Haifa, Israel*

[3]*Institute for Mathematics, Carl von Ossietzky University of Oldenburg, P.F 2503, 26111 Oldenburg, Germany*

(Received 19 December 2016; published 2 June 2017)

Ionic liquids are solvent-free electrolytes, some of which possess an intriguing self-assembly at finite length scale due to Coulombic interactions. Using a continuum framework (based on Onsager's relations), it is shown that bulk nanostructures arise via linear (supercritical) and nonlinear (subcritical) bifurcations (morphological phase transitions), which also directly affect the electrical double layer structure. A Ginzburg-Landau amplitude equation is derived and the bifurcation type is related to model parameters, such as temperature, potential, and interactions. Specifically, the nonlinear bifurcation occurs for geometrically dissimilar ions and, surprisingly, is induced by perturbations on the order of thermal fluctuations. Finally, qualitative insights and comparisons to the experimentally decaying charge layers within the electrical double layer are discussed.

DOI: 10.1103/PhysRevE.95.060201

Solvent-free ionic liquids (ILs) are comprised of large and asymmetric anions and cations, with their molecular structure consisting of a charged ion attached to a hydrophilic or hydrophobic functional group. With significant charge delocalization and irregular geometries, the ions do not readily form a tightly bound lattice and remain liquid even at room temperatures [1]. Their tunable molecular structure enables the tailoring of ILs to a large number of applications [2–9], e.g., batteries, supercapacitors, dye-sensitized solar cells, lubricants, and nanoparticle syntheses, where they are advantageous due to their high charge density, low volatility, and high chemical, thermal, and electrochemical stability.

It is the amphiphilic-type structure, however, that gives ILs another intriguing property—the ability to *self-assemble* (see [10], and references therein). IL molecules spontaneously form bicontinuous, hexagonal or lamellar phases (see [11], and references therein), in a fashion similar to the morphologies of diblock copolymers and liquid crystals. The bulk nanostructure affects not only the mechanical and transport properties [12], but also the electrical double layer (EDL) structure and thus charge-transfer properties [13–16]. Obtaining insight into the emergence of nanostructures is therefore essential for the integration and control of ILs in scientific and industrial applications [2–5,8,9,16].

It was recently shown theoretically that the coupling of bulk and EDL morphologies may be portrayed as the result of competition between short-range intermolecular interactions (e.g., hydrophobic interactions, hydrogen bonds, steric effects) and the long-range Coulombic interactions [17], where the contribution of the former may be incorporated via the Cahn-Hilliard theory of phase separation. This nonlocal Cahn-Hilliard framework has successfully reproduced the emergence of bulk nanomorphologies that have been observed experimentally [10,11], while providing further insights into electrokinetic phenomena in ILs, namely, in the form of transient currents. However, the methodology was based on geometrically identical ions, which is clearly an approximation of any real-world system [11]. Concerning the EDL, recent works have implied that changes of charge layering should be attributed to electrode polarization [15] while ignoring the bulk nanostructure. However, it is difficult to determine solely on the basis of experiments [18,19] and atomistic-type simulations [20,21] whether EDL structure depends on the specific electrode polarization or whether it is generic. Isolating the influences of the bulk and interface properties is challenging as the coupling between them is inherent in the system [17], and measurements of the EDL alone may lead to erroneous conclusions about the bulk, namely, that observations of decaying charge layering in the EDL immediately implies an unstructured bulk [22]. While the coupling between morphology and Coulombic forces has been outlined in [17], the generic features of morphological transitions and their respective impacts on EDL structure remain open [11,18].

Here we focus on a nonlinear theory of asymmetric ionic liquids near the finite wave number onset by first deriving a Ginzburg-Landau amplitude equation and then using a numerical continuation method to distinguish between the linear and the nonlinear instabilities. The distinct emerging solutions are shown to account for the nanomorphology both in the bulk and in the EDL. Particularly, we show that the formation of ordered layers near the solid surfaces is induced by natural energy fluctuations, while the observed decaying spatial charge oscillations may be attributed to an isotropic bulk morphology (independent of the instability type), rather than an unstructured bulk. As such, morphological transitions have fundamental implications to electrochemical charge transport and transfer.

Following [17] and the Onsager framework [23,24], the equations of motion for a fully dissociated and solvent-free IL of monovalent anions ($0 \leqslant n \leqslant n_{\max}$) and cations ($0 \leqslant p \leqslant p_{\max}$) molar concentrations, read as

$$\frac{\partial}{\partial t}\begin{pmatrix} p \\ n \end{pmatrix} = \frac{M}{\bar{c}}\nabla\left[pn\begin{pmatrix} \gamma & -1 \\ -1 & 1/\gamma \end{pmatrix}\nabla\begin{pmatrix} \delta\mathcal{E}/\delta p \\ \delta\mathcal{E}/\delta n \end{pmatrix}\right], \tag{1}$$

*ngavish@tx.technion.ac.il
†yochelis@bgu.ac.il

where M is the diffusion coefficient [25–27] and $\gamma = p_{\max}/n_{\max} > 0$ is the packing ratio of the ions affected by their geometry, and the free energy

$$\mathcal{E} = \int_\Omega d\mathbf{r}\Big\{k_B T\Big[p\ln\frac{p}{\bar{c}} + n\ln\frac{n}{\bar{c}}\Big] + \frac{\bar{c}\beta}{p_{\max}n_{\max}}np + \frac{E_0\kappa^2\bar{c}}{4}\Big(\Big|\frac{\nabla p}{p_{\max}}\Big|^2 + \Big|\frac{\nabla n}{n_{\max}}\Big|^2\Big) + q\bar{c}(p-n)\phi - \frac{1}{2}\epsilon|\nabla\phi|^2\Big\},$$

where $\bar{c}$ is the harmonic average density of ions, k_B is the Boltzmann constant, T is the temperature, β is the interaction parameter for the anion-cation mixture and has units of energy, $E_0\kappa^2/4$ is the interfacial energy coefficient where E_0 has units of energy and κ has units of length, ϕ is the electric potential, q is the elementary charge, and ϵ is the permittivity. Notably, due to the interaction parameters β and κ, the above free energy goes beyond the Poisson-Nernst-Planck (PNP) formulation, and rather gives rise to a nonlocal Cahn-Hilliard framework. These parameters originate from the Flory-Huggins mixture theory, and account for the anion and cation short-range interactions (e.g., hydrophobic interactions and steric interactions). The link between the free energy of ion interactions via a short-range (Lennard-Jones type) potential and the parameter β was presented in [28].

Next, we introduce nondimensional variables and parameters $\tilde{p} = p/p_{\max}$, $\tilde{n} = n/n_{\max}$, $\tilde{\mathbf{x}} = \mathbf{x}/\lambda$, $\tilde{t} = t/\tau$, $\tilde{\phi} = q/(k_BT)\phi$, $\lambda = \sqrt{\gamma\epsilon k_BT/[(1+\gamma)q^2c_{\max}]}$, $\tau = \lambda^2/[(1+\gamma)K_BT]$, and obtain (after omitting the tildes) the final dimensionless equations for the asymmetric ILs:

$$\partial_t p = \nabla\Big[\Big(1 + \frac{1-\gamma}{\gamma}p\Big)\nabla p + p(1-p) \times \Big(\frac{1+\gamma}{\gamma}\nabla\phi - \frac{2\chi}{1+\gamma}\nabla p - \frac{2\sigma}{1+\gamma}\nabla^3 p\Big)\Big], \quad (2a)$$

$$\nabla^2\phi = 1 - (1+\gamma)p, \quad (2b)$$

with $\partial_t n = -\gamma^{-1}\partial_t p$. The parameter $\sigma = \frac{E_0}{2k_BT}\frac{\kappa^2}{\lambda^2}$ depends on the ratio of the strengths of short- and long-range interactions and reflects the competition between them, and $\chi = \beta/(k_BT)$ is the Flory parameter. For consistency with traditional dimensionless analysis, we have chosen to scale space by the Debye-like scale λ while noting that this choice does not reflect a typical electric screening length, as for dilute electrolytes.

Numerical solutions of (2) [29], however, show that unlike the symmetric case $\gamma = 1$ [17], the emergence of spatially inhomogeneous solutions for $\gamma \neq 1$ are of either small or large amplitude states. These results are depicted in Fig. 1 and indicate that the more realistic situation of asymmetric ILs involves both linear and nonlinear instabilities, as we show next. Notably, these instabilities have the nature of type-II and type-I phase transitions, respectively. However, unlike the spinodal-binodal transitions known from thermodynamic theory of binary fluids and associated with long wave-number instabilities [30,31], here self-assembly involves a persistent typical length scale due to coupling to Coulombic interactions [17,32,33]. For the sake of analysis, we first consider an infinite

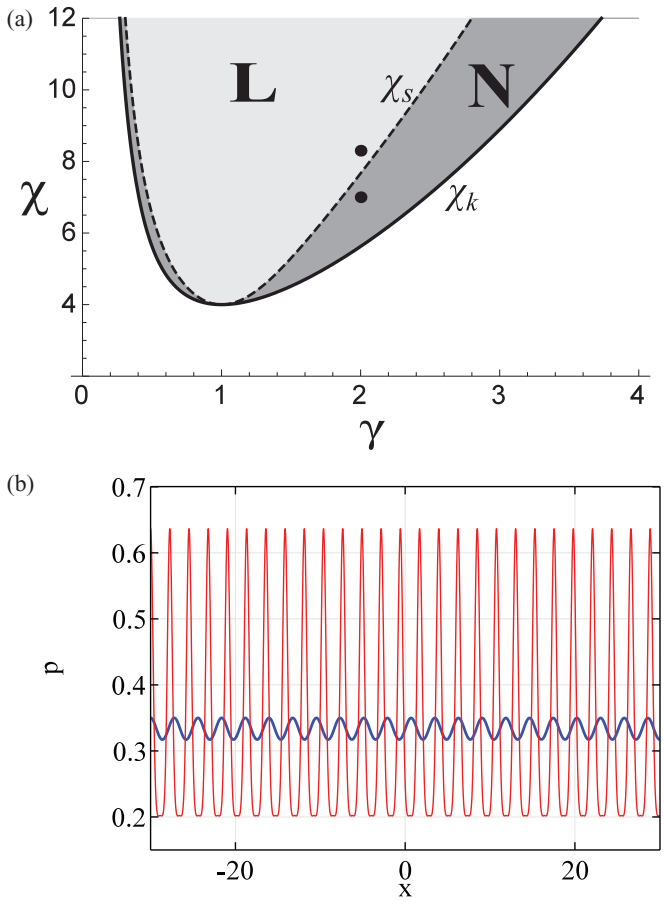

FIG. 1. (a) Parameter space spanned by (γ,χ) in which the system undergoes linear (L, supercritical) and nonlinear (N, subcritical) bulk instabilities at $\sigma = \sigma_c$. The critical lines χ_k and χ_S are given by (5) and (8), respectively. (b) Asymptotic charge profiles obtained by direct numerical integration of (2) for $\chi = 8.3$ [small amplitude solution with dark (blue) line] and $\chi = 7$ [large amplitude solution with light (red) line] at $\gamma = 2$ and $(\sigma - \sigma_c)/\sigma_c = -0.001$, as also marked by solid circles in (a), respectively; initially $p(x,t=0) = p_0$ and $\phi(x,t=0) = 0$ with effective no-flux boundary conditions were employed for all variables except $\phi(L=30) = 0$, with $2L$ being the domain size.

domain in one space dimension (1D), using σ as a control parameter. We then proceed to demonstrate the validity of the results on a finite domain $x \in (-L,L)$ as well, using no-flux (i.e., Neumann) boundary conditions for p, and fixed potential (i.e., Dirichlet) boundary conditions $\phi(x = \pm L) = \pm V/2$, where V is the applied potential difference.

To divine the nature of bulk instabilities, we employ the weakly nonlinear theory (multiple time scale analysis) [34]

$$\begin{pmatrix} p \\ \phi \end{pmatrix} = \begin{pmatrix} p_0 + \epsilon^{1/2}p_1 + \epsilon p_2 + \epsilon^{3/2}p_3 + \cdots \\ \epsilon^{1/2}\phi_1 + \epsilon\phi_2 + \epsilon^{3/2}\phi_3 + \cdots \end{pmatrix}, \quad (3)$$

where $p_0 = 1/(1+\gamma)$ is the uniform cation concentration, $\epsilon \ll 1$ measures the distance from the instability onset, and following [32,33]

$$p_1 = A(\epsilon t, \sqrt{\epsilon}x)e^{ik_cx} + \text{complex conjugate},$$

and $\phi_1 = p_1/(p_0k_c^2)$. The complex amplitude A describes slow variations in space and time, and k_c is the critical wave

number at the instability onset $\epsilon := (\sigma - \sigma_c)/\sigma_c = 0$. Both quantities are obtained by analysis of linear stability to periodic perturbations about the uniform state $(p,\phi) = (p_0,0)$ [34]. Linearizing (2) around $(p_0,0)$, i.e., setting $p = p_0 + P$ and retaining linear terms in (P,ϕ), yields

$$\frac{\partial P}{\partial t} = \frac{\partial}{\partial x}\left[\frac{1+\gamma^2}{\gamma(1+\gamma)}\frac{\partial P}{\partial x} - \frac{\gamma}{(1+\gamma)^2}\left(\frac{2\chi}{1+\gamma}\frac{\partial P}{\partial x} + \frac{2\sigma}{1+\gamma}\frac{\partial^3 P}{\partial x^3}\right)\right] + \frac{1}{1+\gamma}\frac{\partial^2\phi}{\partial x^2},$$

$$\frac{\partial^2\phi}{\partial x^2} = -(1+\gamma)P,$$

and substituting the second into the first equation yields the dispersion relation of finite wave-number instability type [17]

$$s = -1 + \left[\chi\frac{2\gamma}{(1+\gamma)^3} - \frac{1+\gamma^2}{\gamma(1+\gamma)}\right]k^2 - \sigma\frac{2\gamma}{(1+\gamma)^3}k^4. \tag{4}$$

We note that there is a factor of 2 which appears due to using the molar concentration rather than a volume fraction that was used in [17]. In (4), s is the temporal growth rate of periodic perturbations associated with finite wave numbers k, i.e., $s(k) > 0$ implies linear instability. Varying σ, the instability onset is obtained by seeking $\sigma = \sigma_c$ and k_c such that $s(k_c) = 0$, $s(k \neq k_c) < 0$ and $\frac{ds}{dk}(k_c) = 0$, yielding

$$\sigma_c = \frac{[2\gamma^2\chi - (1+\gamma^2)(1+\gamma)^2]^2}{8\gamma^3(1+\gamma)^3}, \quad k_c^2 = \sqrt{\frac{(1+\gamma)^3}{2\sigma_c\gamma}}.$$

Notably, although the model equations are gradient, the coupling to the Poisson equation damps the large-scale mode [17,32,33], i.e., $s(0) < 0$. Since $k_c^2, \gamma > 0$, the instability may exist only for

$$\chi > \chi_k = \frac{(1+\gamma^2)(1+\gamma)^2}{2\gamma^2}, \tag{5}$$

as identified by the shaded region in Fig. 1. For the symmetric case ($\gamma = 1$) we retain the result $\chi_k = \chi_c \equiv \beta_c/(k_B T) = 4$ from [17].

Slightly above the instability onset, $\epsilon \ll 1$, the dispersion relation admits a finite band of wave numbers around k_c for which $s > 0$. However, direct numerical integration shows that at $\epsilon = -0.001$ and $\gamma = 2$, we find two distinct cases: for $\chi = 8.3$ the solutions correspond to small amplitude periodic solutions [see dark line in Fig. 1(b)], while for $\chi = 7$ the solutions are highly nonlinear [as evidenced by the spikelike shape of the light line in Fig. 1(b)] and of large amplitude (relative to ϵ). This behavior indicates two types of instability mechanisms, which can be analyzed using the amplitude equation for A. Thus we substitute (3) into (2), and after imposing the solvability condition at order $\epsilon^{3/2}$ obtain

$$\frac{\partial A}{\partial t} = \frac{\sigma_c - \sigma}{\sigma_c}A + \alpha|A|^2 A + \frac{4}{k_c^2}\frac{\partial^2 A}{\partial x^2}, \tag{6}$$

where $\alpha = (1+\gamma)^2/\gamma + k_c^2(2\sigma_c k_c^2 - 2\chi)/(1+\gamma) + \frac{2(\gamma^3-1)k_c^2}{9\gamma}[\frac{\gamma^2-1}{2\gamma} - (\frac{1-\gamma}{\gamma} + \frac{2\chi(1-\gamma)}{(1+\gamma)^2})k_c^2 + 7\frac{2\sigma_c(1-\gamma)}{(1+\gamma)^2}k_c^4]$. The Ginzburg-Landau partial differential amplitude equation (6) can be used to approximate large-scale modulations of the basic pattern $\cos(k_c x + \varphi)$ near the instability onset [32,33] but here for simplicity we assume A to be independent of space and $\varphi = 0$. Then

$$p \simeq \frac{1}{1+\gamma} + 2\sqrt{\frac{\sigma - \sigma_c}{\sigma_c\alpha}}\cos k_c x, \tag{7a}$$

$$\phi \simeq 2\frac{1}{p_0 k_c^2}\sqrt{\frac{\sigma - \sigma_c}{\sigma_c\alpha}}\cos k_c x. \tag{7b}$$

From the right-hand sides of (7) it is evident that the signs of $\sigma - \sigma_c(\gamma,\chi)$ and of $\alpha(\gamma,\chi)$ differentiate between two types of periodic solutions: (i) the supercritical bifurcation when $\sigma < \sigma_c$ and $\alpha < 0$, with the amplitude scaled as $\sqrt{|\sigma - \sigma_c|}$ [see Fig. 2(a)], and (ii) the subcritical (nonlinear) bifurcation when $\sigma > \sigma_c$ and $\alpha > 0$, with the amplitude exhibiting a discontinuous jump to amplitudes $O(1)$ for $\sigma < \sigma_c$. Typical solutions of both cases for $\sigma \lesssim \sigma_c$ obtained via direct numerical integration are depicted in Fig. 1(b), while the transition between the two types is obtained by solving for $\alpha(\chi,\gamma) = 0$, which yields

$$\chi_s = \{\gamma[\gamma(\gamma\{\gamma[\gamma(13\gamma - 9) + 18] - 26\} + 27) - 9] + 22\} \times \frac{(\gamma+1)^2}{18\gamma^2[\gamma(\gamma-1)(\gamma^2+1) + 2]}, \tag{8}$$

as depicted by the dashed line in Fig. 1(a).

The branches of bifurcating solutions beyond the weakly nonlinear limit are computed in both cases with a numerical continuation method [35], as depicted in Fig. 2. While in the supercritical (linear) case the bifurcating periodic solutions are stable [Fig. 2(a)], in the subcritical case (nonlinear) these solutions are linearly unstable until reaching a fold, σ_c^{SN}, whereon they change direction and grow toward the instability onset of the homogeneous state. However, as in the Ohta-Kawasaki case [33], the large amplitude periodic solutions belonging to a branch portion after the fold ($\sigma < \sigma_{SN}$; see figure) are stable on $2L = \lambda_c = 2\pi/k_c$ (exhibiting hysteresis) but become Eckhaus unstable on large domains; due to applications our interest here is in domains that are larger than the wavelength of the bifurcating states, i.e., $L \gg \pi/k_c$. Consequently, the hysteresis region $\sigma_c < \sigma < \sigma_c^{SN}$, between the k_c solutions and the uniform state is destroyed on large domains. Nevertheless, direct numerical integration shows that there are additional periodic solutions that emerge and form hysteresis for $\sigma_c < \sigma < \sigma_L^{SN}$ [Fig. 1(b)]. These solutions belong to one of the secondary branches of periodic solutions (denoted by k_L) that emerge below the onset, i.e., at $\sigma < \sigma_c$ as shown by thick line in Fig. 2(b).

From a mathematical point of view, bistability of the uniform and periodic states persist on finite domains. However, in the physical context, perturbations are related to energy fluctuations which operate at the scale of $k_B T$ or $\phi \sim 1$ in dimensionless units. The size of fluctuations should be compared to the amplitude of the unstable parts of the subcritical branches, i.e., $\sigma_c < \sigma < \sigma_{c,L}^{SN}$. Setting $\phi \approx 1$ in (7b) yields

$$\sigma - \sigma_c > \left|\frac{\alpha\sigma_c p_0^2 k_c^4}{4}\right| \sim \frac{32}{\chi - 4} + O(\gamma - 1). \tag{9}$$

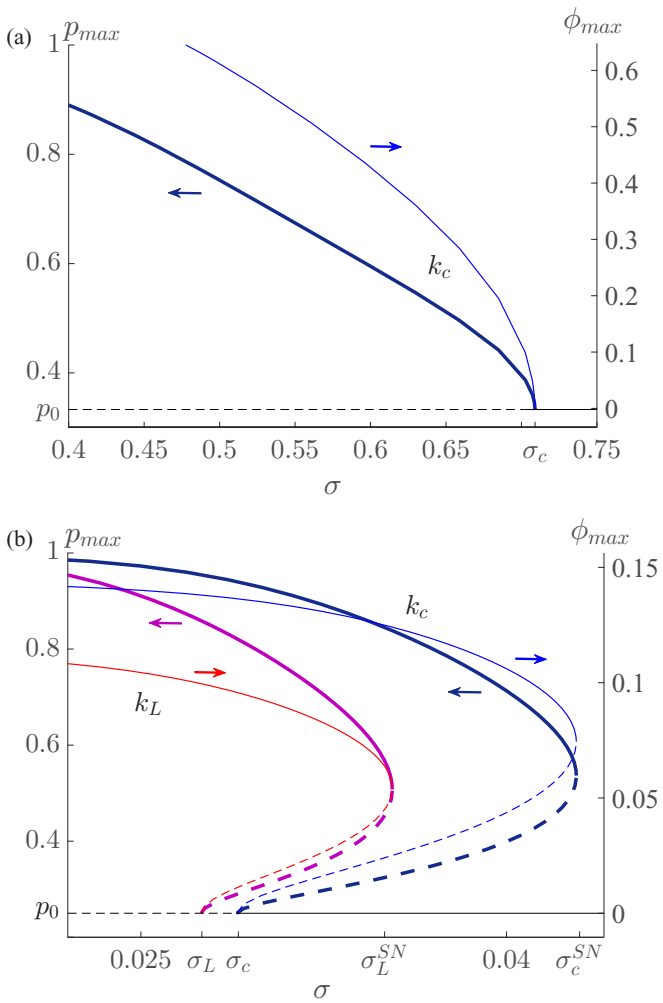

FIG. 2. Bifurcation diagrams for (a) $\sigma < \sigma_c, \alpha < 0$ and (b) $\sigma > \sigma_c, \alpha > 0$, showing the maximal values, $p_{\max} = \max|p|$ (thick curves and left arrows) and $\phi_{\max} = \max|\phi|$ (thin curves and right arrows), of the bifurcating periodic solutions as a function of σ. The (a) super- and (b) subcritical branches have been obtained using numerical continuation via the PDE2PATH package [35]; solid (dashed) curves mark stable (unstable) solutions along the branches. The k_c branch in (b) corresponds to a single-period domain size ($2L = 2\pi/k_c$), with $k_c \simeq 4.382$, $\sigma_c \simeq 0.029$, $\sigma_c^{SN} \simeq 0.043$, while the k_L branch with $k_L \simeq 5$, $\sigma_L \simeq 0.027$, and $\sigma_L^{SN} \simeq 0.035$ is one of the branches obtained for a large domain ($2L = 100$).

The numerical continuation in Fig. 2(b) shows that in the parameter regimes considered here, the folds $\sigma_{c,L}^{SN}$ are too close to σ_c for (9) to overcome thermal fluctuations, i.e., $\phi(\sigma_{c,L}^{SN}) \simeq 0.05 \ll 1$ or about 5% of thermal energy. Indeed, even weak perturbations $\phi(\pm L) = \pm V$ with $|V| \ll 1$ at the boundaries give rise to a large-amplitude pattern, as shown in Fig. 3. In other words, in a physicochemical system with the required temperature and anion-cation asymmetry, energy fluctuations will drive the formation of large amplitude nanostructures for $\sigma_c < \sigma < \sigma_L^{SN}$, even though the homogeneous state is linearly stable.

The weakly nonlinear analysis indicates that the asymmetric IL model (2) belongs to a universality class described by the Ginzburg-Landau equation, which includes both conserved

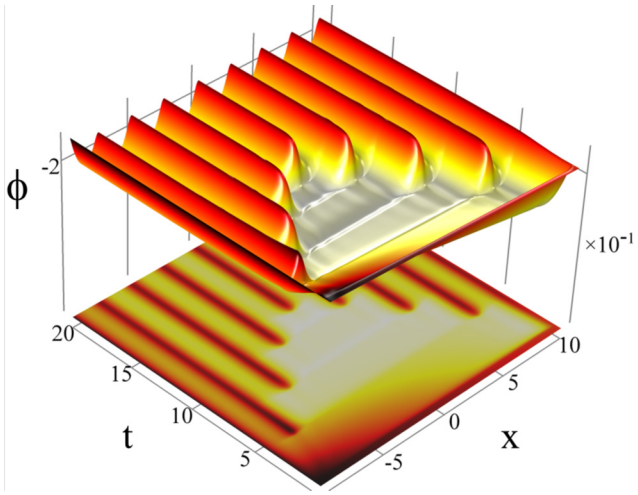

FIG. 3. Space-time plot showing the formation of large amplitude solutions from a weak perturbation at the boundaries, $\phi(x = \pm L) = \pm 0.01$. The top panel shows the profile of ϕ as a surface while the bottom panel as a contour with initially $p(x) = p_0 = 1/(1+\gamma)$ and $\phi = 0$. Parameters: $\gamma = 3$, $\chi = 10$, $L = 10$, $(\sigma - \sigma_c)/\sigma_c = 0.1$.

and dissipative systems, such as Swift-Hohenberg, reaction-diffusion, and nonlocal Cahn-Hilliard equations. Consequently, based on pattern formation theory [31,34] and the related nonlocal Ohta-Kowasaki model [33,36] it is evident that the large amplitude periodic patterns in the one-dimensional (1D) asymmetric IL model (2) will take on much richer universal forms in 2D and 3D, such as laminar, bicontinuous, and spongelike morphologies [36–39]; systematic study of patterns in higher dimensions is beyond the scope of this Rapid Communication. In particular, nonlocal Cahn-Hilliard theory shows that 1D periodic bulk structures exhibit universal behavior, manifesting as labyrinthine and hexagonal patterns in 2D and 3D [31,34] (e.g., Fig. 4(c) in [17]). The former pattern may be expected in the region of subcritical bifurcations for nearly symmetric cases ($\gamma \approx 1$) and emerge via a zigzag instability [17], while the latter emerges in asymmetric systems ($|\gamma - 1| \gg 0$) via a subcritical bifurcation [31,36]. Indeed, the early experimental observations have used protic IL with short alkyl groups that correspond to $\gamma \approx 1$ [40].

Commonly used experimental measurements such as atomic force microscopy [41], atomic force apparatus [42], and x-ray reflectivity [14] cannot distinguish between a uniform bulk and a nanostructured bulk that emerged via either type of instability. This is because these experimental measurements are essentially one-dimensional methods measuring the spatial average of the system (system projection on the parallel axis) on planes parallel to the electrodes. A nanostructured bulk, in which a convoluted periodic morphology emerges due to thermal fluctuations, will average out to electroneutrality on planes parallel to the boundary [17,43], and thus bulk structure will remain undetected. The distinction between a structured and unstructured bulk may be further advanced, for example, using time-dependent measurement which shows different behavior in each case [17].

To conclude, we have demonstrated the generic nature of self-assembly in both the bulk and the electrical double layer regions of asymmetric ionic liquids. The nanomorphology is

shown to arise first in the bulk via linear or nonlinear instabilities, following the derived Ginzburg-Landau amplitude equation (6). In both types, near the onset, σ_c, the bulk is sensitive to energy fluctuations of about k_BT or, respectively, 25 mV, with the resulting formation of large amplitude nanomorphologies even in the subcritical (linearly stable bulk) case. Since these instabilities are of universal nature [31,34], in higher space dimensions the morphologies that form are isotropic (e.g., labyrinths and hexagons) and thus, averaging about the plane parallel to the electrodes will yield results that seem to correspond to a uniform density with a vanishing electrical field, i.e., electroneutrality in the 1D context. The second effect of an isotropic structured bulk is its subtle impact on the charge layering within the EDL region [10,11]. Since the bulk isotropy breaks down near the solid surface, the patterns tend to align with electrode orientation [17]. Upon averaging about the plane normal to the electrode one naturally observes charge layers near the electrode that gradually lose their orientation toward the bulk, cf. [43]. Consequently, spatially decaying oscillations are observed in the direction normal to the electrode, yet they should not be misinterpreted as evidence for the absence of bulk self-assembly. As many applications [11,16], e.g., energy- and lubrication-related, exploit and depend on mass transport and charge transfer properties, the framework developed here offers another perspective regarding the interpretation of empirical observations, as well as opportunities for the enhancement of device efficiency [2–9] in terms of conductivity, structural integrity (rheology), and electrochemical reactions.

This research was done in the framework of the Grand Technion Energy Program (GTEP) and of the BGU Energy Initiative Program, and supported by the Adelis Foundation for renewable energy research. N.G. acknowledges also the support from the Technion VPR fund and from EU Marie-Curie CIG Grant No. 2018620.

[1] J. Dupont, Acc. Chem. Res. **44**, 1223 (2011).
[2] N. V. Plechkova and K. R. Seddon, Chem. Soc. Rev. **37**, 123 (2008).
[3] D. S. Silvester and R. G. Compton, Z. Phys. Chem. (Muenchen) **220**, 1247 (2006).
[4] J. Wishart, Energy Environ. Sci. **2**, 956 (2009).
[5] F. Zhou, Y. Liang, and W. Liu, Chem. Soc. Rev. **38**, 2590 (2009).
[6] A. Brandt, S. Pohlmann, A. Varzi, A. Balducci, and S. Passerini, MRS Bull. **38**, 554 (2013).
[7] Q. Li, Q. Tang, B. He, and P. Yang, J. Power Sources **264**, 83 (2014).
[8] D. MacFarlane, M. Forsyth, E. Izgorodina, A. Abbott, G. Annat, and K. Fraser, Energy Environ. Sci. **7**, 232 (2014).
[9] M. Armand, F. Endres, D. MacFarlane, H. Ohno, and B. Scrosati, Nat. Mater. **8**, 621 (2009).
[10] A. Yochelis, M. B. Singh, and I. Visoly-Fisher, Chem. Mater. **27**, 4169 (2015).
[11] R. Hayes, G. G. Warr, and R. Atkin, Chem. Rev. **115**, 6357 (2015).
[12] A. Erbas and M. O. de la Cruz, Phys. Chem. Chem. Phys. **18**, 6441 (2016).
[13] F. Endres, O. Höfft, N. Borisenko, L. Gasparotto, A. Prowald, R. Al-Salman, T. Carstens, R. Atkin, A. Bund, and S. Zein El Abedin, Phys. Chem. Chem. Phys. **12**, 1724 (2010).
[14] A. Uysal, H. Zhou, G. Feng, S. S. Lee, S. Li, P. Fenter, P. T. Cummings, P. F. Fulvio, S. Dai, J. K. McDonough *et al.*, J. Phys. Chem. C **118**, 569 (2013).
[15] B. Rotenberg and M. Salanne, J. Phys. Chem. Lett. **6**, 4978 (2015).
[16] M. V. Fedorov and A. A. Kornyshev, Chem. Rev. **114**, 2978 (2014).
[17] N. Gavish and A. Yochelis, J. Phys. Chem. Lett. **7**, 1121 (2016).
[18] N. Hjalmarsson, R. Atkin, and M. W. Rutland, Chem. Commun. **53**, 647 (2017).
[19] F. Lo Celso, Y. Yoshida, F. Castiglione, M. Ferro, A. Mele, C. J. Jafta, A. Triolo, and O. Russina, Phys. Chem. Chem. Phys. **19**, 13101 (2017).
[20] R. M. Lynden-Bell, A. Frolov, and M. V. Fedorov, Phys. Chem. Chem. Phys. **14**, 2693 (2012).
[21] C. Merlet, D. T. Limmer, M. Salanne, R. Van Roij, P. A. Madden, D. Chandler, and B. Rotenberg, J. Phys. Chem. C **118**, 18291 (2014).
[22] M. Z. Bazant, B. D. Storey, and A. A. Kornyshev, Phys. Rev. Lett. **106**, 046102 (2011).
[23] L. Onsager and R. Fuoss, J. Phys. Chem. **36**, 2689 (1932).
[24] J. E. Hilliard, in *Phase Transformations*, edited by H. I. Aaronson (ASM, Metals Park, Ohio, 1970).
[25] P. De Gennes, J. Chem. Phys. **72**, 4756 (1980).
[26] F. Brochard, J. Jouffroy, and P. Levinson, Macromolecules **16**, 1638 (1983).
[27] S. Psaltis and T. W. Farrell, J. Electrochem. Soc. **158**, A33 (2011).
[28] T.-C. Lin and B. Eisenberg, Commun. Math. Sci. **12**, 149 (2014).
[29] Direct numerical integrations were performed using the commercial software COMSOL 5.2.
[30] L. M. Pismen, *Patterns and Interfaces in Dissipative Dynamics* (Springer-Verlag, Berlin, 2006).
[31] A. A. Golovin and A. A. Nepomnyashchy (eds.), *Self-Assembly, Pattern Formation and Growth Phenomena in Nano-Systems*, Proceedings of the NATO Advanced Study Institute, St. Etienne de Tinee, France (Springer Science & Business Media, New York, 2006), Vol. 218.
[32] Y. Shiwa, Phys. Lett. A **228**, 279 (1997).
[33] N. Gavish, I. Versano, and A. Yochelis, SIAM J. Appl. Dyn. Syst., doi:10.1137/16M1105876.
[34] M. C. Cross and P. C. Hohenberg, Rev. Mod. Phys. **65**, 851 (1993).
[35] H. Uecker, D. Wetzel, and J. Rademacher, Numer. Math.-Theory Methods Appl. **7**, 58 (2014), see also www.staff.uni-oldenburg.de/hannes.uecker/pde2path/
[36] R. Choksi, M. A. Peletier, and J. Williams, SIAM J. Appl. Math. **69**, 1712 (2009).
[37] I. A. Nyrkova, A. R. Khokhlov, and M. Doi, Macromolecules **27**, 4220 (1994).

[38] U. Thiele, A. J. Archer, M. J. Robbins, H. Gomez, and E. Knobloch, Phys. Rev. E **87**, 042915 (2013).
[39] H. Uecker and D. Wetzel, SIAM J. Appl. Dyn. Syst. **13**, 94 (2014).
[40] R. Atkin and G. Warr, J. Phys. Chem. B **112**, 4164 (2008).
[41] R. Atkin, N. Borisenko, M. Drüschler, F. Endres, R. Hayes, B. Huber, and B. Roling, J. Mol. Liq. **192**, 44 (2014).
[42] S. Perkin, Phys. Chem. Chem. Phys. **14**, 5052 (2012).
[43] K. Lazaridis, L. Wickham, and N. Voulgarakis, Phys. Lett. A **381**, 1431 (2017).